

# A CMOS Motion Detector System for Pointing Devices

Xavier Arreguit, F. André van Schaik, *Student Member, IEEE*, François V. Bauduin, Marc Bidiville, and Eric Raeber

**Abstract**— A motion detector system uses an array of 93 photodiodes integrated along with processing circuits to detect the motion of a printed random pattern on a ball used in a pointing device application. It is based on the detection and tracking of spot edges passing over a matrix of pixels during the period between two light pulses. Motion in  $x$  and  $y$  directions is estimated by aggregating local information about moving edges over the photosensitive pixels. The  $4.4 \times 4.3 \text{ mm}^2$  chip detects the ball motion from 0 to 11.8 in/s with a resolution higher than 800 dpi over a 100–2000  $\text{mW/m}^2$  light-intensity range.

## I. INTRODUCTION

**O**PTICAL motion detection of a moving ball with a printed pattern on its surface overcomes the foregoing limitations of the prior art of pointing devices by eliminating entirely the use of mechanical parts like the shaft encoders and their associated encoding wheels and rollers. Optimization of the pointing device microsystem as a whole, taking into account size, power consumption, and cost limitations to ensure simple manufacturability, imposes constraints on its different components that will not necessarily result in an optimum for each component. Simplicity of the printed pattern on the ball, low power consumption and small chip size considerations have driven the design of the CMOS motion detector sensor presented in this paper.

Several solutions have been proposed in the past for the design of optical pointing devices such as the mouse or the trackball based on an image sensor [1]–[6]. R. F. Lyon developed an innovative optical mouse design that integrated sensors along with the processing onto the same chip. His design required a particular working surface consisting of a hexagonal grid of light dots on a dark background and the comparison of successive snapshots providing a sequence of bitmaps that can be interpreted in terms of direction and amount of movement. To relax the requirements on the working surface, other correlation techniques have been developed, based on the comparison of two images stored at two different times shifted with respect to each other [3]. This solution requires to quantize and to store digitally the image, before computing the correlation between shifted versions of the stored image and the current one to determine the direction

of greatest correlation as the direction of the movement. Any regular or irregular grey-scale pattern can therefore be used as an operating surface. However, quantization can result in a problem in the presence of illumination gradients added to the image and resolution is limited to the pitch between photodiodes. Circumventing previous limitations, J. Tanner has developed an attractive solution [4]. His circuit uses analog values of intensity of any kind of printed pattern to compute velocity continuously. Based on analog circuits integrated alongside the photodiodes, it extracts the velocity of the image from locally measured derivatives, and aggregates local information to compute a global result taking advantage of analog collective computation. Although this solution circumvents previous limitations, it is still unsuitable for our intended application from the point of view of power consumption, since it requires continuous illumination of the surface, which draws most of the microsystem power consumption.

The approach we present in this paper is improving on the performances of the previously proposed solutions by reducing the system power consumption by at least two orders of magnitude, by increasing the tracking resolution to above 800 dpi, and by requiring only a randomly-sized, -shaped and -positioned two-level intensity pattern printed on the surface of the ball instead of a precise regular pattern.

The next section describes the microsystem and resulting specifications and constraints on the chip. Section III presents the principle used for estimating the direction and speed of motion of the ball and Section IV discusses some particular points of interest about circuit design and on-chip test considerations. A performance summary will be presented before drawing conclusions.

## II. MICROSYSTEM DESCRIPTION: CONSTRAINTS AND SPECIFICATIONS

Fig. 1 shows the different components of an optical motion detection microsystem. It is composed of a ball with a printed pattern of spots that contrasts with the background color; LED's to illuminate part of the ball; a lens to focus an image onto the surface of the chip; a CMOS chip composed of an array of photodetectors and processing circuits outputting signals converted to two 5-b digital words fed to a microprocessor that establishes the protocol for communications with the personal computer and generates required interrupts.

Optimizing a microsystem in terms of size, cost, power consumption, and manufacturability requires tradeoffs for establishing the component specifications and imposes some constraints on the design of the chip. In particular, to simplify

Manuscript received May 17, 1996; revised August 19, 1996.

X. Arreguit and F. V. Bauduin are with CSEM Centre Suisse d'Electronique et de Microtechnique SA, CH-2007 Neuchâtel, Switzerland.

F. A. van Schaik was with CSEM Centre Suisse d'Electronique et de Microtechnique SA, CH-2007 Neuchâtel, Switzerland. He is now with the Swiss Federal Institute of Technology, Lausanne, Switzerland.

M. Bidiville and E. Raeber are with Logitech SA, Romanel/Morges, Switzerland.

Publisher Item Identifier S 0018-9200(96)08409-0.

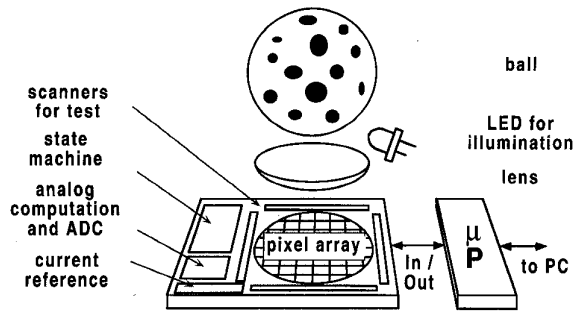


Fig. 1. Pointing device microsystem.

manufacturability of the ball and decrease its cost, the pattern on its surface is composed of random-shape, -position and -size spots. The minimum spot size has been nevertheless specified larger than the pitch between two photodiodes, in order to ensure that its surface projected onto the chip always covers at least one photoreceptor and therefore its tracking is not lost. The minimum ratio between the two reflectances  $R$  on the ball (spot and background) is measured above three, which in terms of optics definition corresponds to a contrast  $(R_{\max} - R_{\min}) / (R_{\max} + R_{\min})$  better than 50%.

For an illumination of the ball specified in the range of 100–500 mW/m<sup>2</sup>, the microsystem overall power consumption is mainly due to the current flowing in the LED (mA-range). To cut power consumption to an average of a few  $\mu$ A, we use a pulsed LED with typically 10- $\mu$ s pulses at a maximum frequency of 1 kHz. This frequency is calculated to comply with the specification of the maximum speed to be detected, i.e., 10 in/s. Moreover, the ball being idle most of the time in normal use, the frequency of illumination is controlled by the microprocessor to reduce power consumption considerably [7].

### III. MOTION DETECTION METHOD

When the ball is moving, spots are displaced over the array of photodetectors. In addition of being sampled in time by the light pulses, the position of a spot is also sampled spatially by the array of photodiodes in the  $x$  and  $y$  directions (300  $\mu$ m pitch). Moving spots at times  $t$  and  $t - 1$  cover two different sets of photodiodes forming different patterns (Fig. 2). Therefore, spatial sampling of random-size and -shape spots makes the use of pattern matching techniques to detect the direction of motion difficult. To circumvent this drawback, a simple solution for motion detection can be devised when observing that, as specified at maximum rotating speed, a spot is never displaced by more than the pitch between photoreceptors during the period between two light pulses, and furthermore that relevant data about displacement of a two-level intensity image during that period is carried essentially by the spot edges passing over photodiodes. For example, in Fig. 2, only photodiodes A through F put out different amounts of photocurrents at times  $t - 1$  and  $t$ . During these two time periods, the ratio between their output current and that of the neighboring photodiodes are different, signalling the motion of an edge.

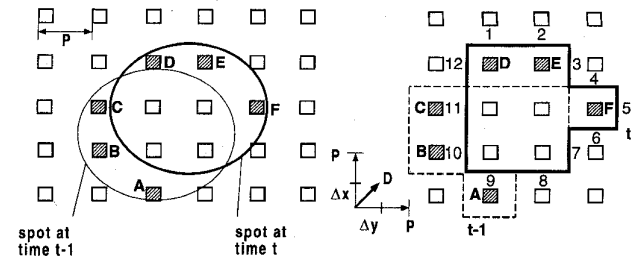


Fig. 2. Spot displacement and detected edges between photodiodes.

For the particular case of a two-level intensity pattern, we define an edge between two photodiodes as occurring when the ratio between their photocurrents is higher than a given factor  $n$  (conversely, lower than a factor  $1/n$ ). This factor must be larger than one to avoid problems related to noise and to the mismatch of analog circuit components, but lower than the minimum measured ratio of three between the two reflectances composing the pattern. Its implementation is discussed in the next section. Detection of an edge is thus a local processing only requiring data between neighboring photodiodes. It is independent of the overall level of a uniform illumination since it is based on the ratio of photocurrents depending upon the product of the ball reflectance and the level of illumination. It is also tolerant to illumination gradients across the photodiode array, providing the variation of illumination level between two neighboring photodiodes is not bigger than the current ratio defining the edge.

Global information about motion of the image is carried by the set of edges moving across the photosensitive array. To derive the displacement components  $\Delta x$  and  $\Delta y$  between two light pulses, let us examine two particular examples. Consider first that a randomly-sized and -shaped spot moves exactly the pitch distance  $P$  between two photodiodes in the  $x$  direction during the period between two light pulses: all vertical edges present between photodiodes laid out in the  $x$  direction must then move by exactly the distance  $P$  in that direction. Consequently, all vertical edges will be reporting moving. Now, consider that a spot is moved by less than the pitch  $P$  ( $\Delta x < P$ ): since the spot edges are randomly distributed over a regular-spaced array of photodetectors, only edges positioned at  $t - 1$  at a shorter distance from a photodiode than the displacement value  $\Delta x$  can move over a photodiode. For example, in Fig. 2, a spot composed of six vertical edges (3, 5, 7, 10, 11, 12) and six horizontal edges (1, 2, 4, 6, 8, 9) at time  $t$  is displaced of  $\Delta x = \Delta y = P/2$ . Between  $t - 1$  and  $t$ , only vertical edges 5, 10, and 11 have moved across their respective photodiode in the  $x$  direction. Horizontal edges 1, 2, and 9 have moved across a photodiode in the  $y$  direction. Provided that the displacement of the focused image of the ball onto the surface of the chip is smaller than the pitch between photodetectors, a good estimation of the displacement between two light pulses in the  $x$ , respectively the  $y$  direction, normalized to the pitch distance  $P$ , is given by the ratio of edges moving in one direction over the total number of edges present between photodiodes laid out in that direction. To simplify the implementation on chip, direction of displacement

can be taken into consideration by subtracting the number of edges moving in one direction from the number of edges moving in the opposite direction

$$\frac{\Delta x}{P} = \frac{\sum R - \sum L}{\sum E_x} \quad (1)$$

$$\frac{\Delta y}{P} = \frac{\sum U - \sum D}{\sum E_y} \quad (2)$$

where  $\sum R$  and  $\sum L$  represent the number of vertical edges moving respectively to the right and to the left,  $\sum U$  and  $\sum D$  represent the number of horizontal edges moving respectively up and down, and  $\sum E_x$  and  $\sum E_y$  represent the total number of vertical and horizontal edges, respectively, detected in the image.

Examining (1) and (2) reveals an interesting property of the presented motion detection method. Because  $\sum E_x$  (respectively  $\sum E_y$ ) are in the denominator, the higher the number of edges, the more resolution we get from the estimations (1) and (2). In other words, by tracking edges of random-position, -shape, and -size spots, the minimum detectable displacement is smaller than the distance between photodiodes, and the resulting subpixel resolution only depends on the total number of edges present on the photosensitive matrix. This is intuitively understood when considering that for edges randomly positioned on the image, the higher the number of edges, the higher the probability that at least one edge is crossing over the photodiode for any given small displacement. This property relaxes the constraints on the minimum pixel size for a specified resolution.

#### IV. SYSTEM AND CIRCUIT DESIGN CONSIDERATIONS

Given a spot density and a pixel size, the number of edges present in the image at a given time, and therefore resolution, can be increased by increasing the size of the ball area focused onto the chip, that is the number of pixels on the photosensitive matrix. For our application, the pitch between photodiodes (pixel size), spot density, and size, as well as the number of pixels in the matrix, have been designed to comply with a tracking resolution higher than 800 dpi. A matrix of only 75 pixels defined in between a 93-photodiodes array is then required, illustrating the fact that a large number of pixels is not always needed for the implementation of low-level vision tasks like motion detection: taking advantage of local and collective processing can result in small size vision chips optimized for a particular task.

To estimate the local displacement of the spots, each pixel is composed of the following parts (Fig. 3):

- an image acquisition circuit composed of a photodiode and a current amplifier captures up to 1000 snapshots of the ball surface per second at the specified illumination level;
- an edge detection block, composed of current mirrors, current comparators, NAND's, and latches detects and stores information about edges at times  $t$  and  $t-1$ ;
- a switch-logic block computes and outputs the local estimate of the displacement.

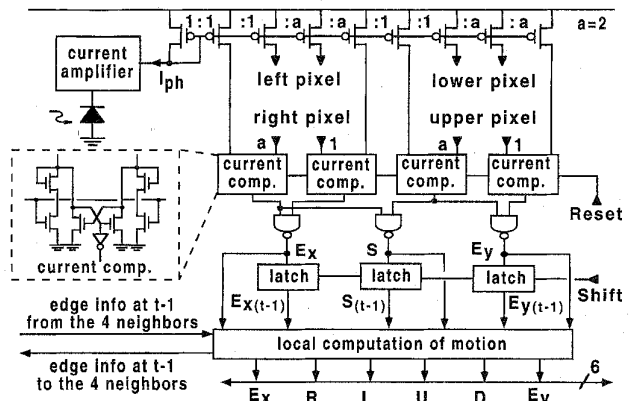


Fig. 3. Pixel block diagram without on-chip test.

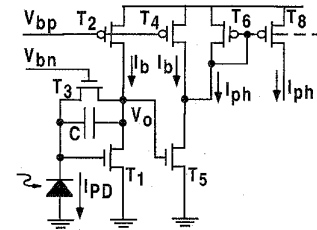


Fig. 4. Image acquisition circuit.

#### A. Image Acquisition

The primary function expected from the image acquisition circuit is to extract reflectance information about the image and output a current which compared to the neighboring currents yields information about spot edges. In the particular case of a two-color image with a minimum ratio between reflectances larger than three, faithful restitution of a grey-scale image is not required as long as information about edges can be preserved and extracted, which relaxes the constraints on circuit precision. However, at the specified illumination conditions (light pulses of 10–20  $\mu\text{s}$  and illumination range of 100–500  $\text{mW}/\text{m}^2$ ), the carriers generated by incident light and collected by a reverse-biased  $n$ -well diode ( $70 \times 70 \mu\text{m}^2$ ) used as a photodetector yield a current too small (less than 1 nA) to drive the input capacitance of the current comparator in the specified time. Amplification of the photodiode current is thus required and is provided by the circuit shown in Fig. 4. Similar to what is done in most CMOS imagers, small currents can be integrated on a small capacitor  $C$  in feedback with a common source amplifier (transistor  $T_1$  loaded by a current source  $I_b$  provided by  $T_2$ ). But instead of periodically switching transistor  $T_3$  to reset the charges across the capacitor before each snapshot, we take advantage in this particular application of the pulsed light to avoid any clock signal in the circuit, thus eliminating charge injection problems on the small capacitor  $C$  of about 40 fF.  $T_3$  is biased with a constant gate voltage which sets its saturation current  $I_{\text{sat}3}$  around 100 pA. When the illumination is switched off, the photocurrent  $I_{\text{PD}}$  is smaller than  $I_{\text{sat}3}$  and  $T_3$  is operating in its conduction mode shorting  $C$ . Drain-source voltage across  $T_3$  sets to allow current  $I_b \gg I_{\text{sat}3}$  to flow through transistor  $T_1$ . When the

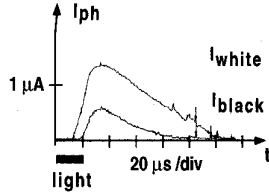


Fig. 5. Typical image acquisition circuit output current.

illumination is turned on, photocurrent  $I_{PD}$  is larger than  $I_{sat3}$  and  $T_3$  enters in saturation mode. Current  $I_{PD} - I_{sat3}$  is then integrated across capacitor  $C$ . Assuming a pulse of current  $I_{PD}$  proportional to the pulse of light, the output voltage can be approximated by

$$V_o(t) = V_o(0) + \frac{1}{C}(I_{PD} - I_{sat3})t. \quad (3)$$

Voltage  $V_o$  is then converted to a current by transistor  $T_5$  from which the bias current  $I_b$  is subtracted to yield  $I_{ph}$ , mirrored by transistors  $T_6$ – $T_{10}$

$$I_{ph} = \frac{\beta_5}{2n} \left( V_o(0) + \frac{1}{C}(I_{PD} - I_{sat3})t - V_T \right)^2 - I_b \quad (4)$$

where  $V_T$  is the transistor threshold voltage,  $\beta_5 = \mu C_{ox} W_5/L_5$ , and  $n$  is the slope factor corresponding to the slope of the  $V_G$  versus pinch-off voltage ( $V_p$ ) characteristic [8]. Fig. 5 shows two measured current outputs for two input currents corresponding to black and white intensity levels in a ratio of two and for a light pulse of 20  $\mu s$ . Notice the delay between the light pulse and the output current pulse due to the diffusion time of carriers actually generated at a depth depending on the light wavelength, with typical penetration depths in the order of few  $\mu m$  for green light and a few tenths of  $\mu m$  for infra-red light, which are larger than the well depth.

Although transistors  $T_1$  and  $T_5$ , respectively  $T_2$  and  $T_4$ , are matched (same dimensions), drain voltage modulation and the voltage across  $T_3$  are designed to provide a current  $I_{T5}$  about 10% larger than current  $I_b$ . This ensures a minimum current to flow in the current mirror  $T_6$ – $T_8$  keeping the transistors saturated, and therefore complies with speed requirements.

### B. Edge Detection and Storage

Copies of  $I_{ph}$  and  $2I_{ph}$  from the pixel amplifier and from the right and upper neighbor amplifiers (Fig. 3) are fed into latched current comparators controlled by the signal “Reset.” “Reset” is turned ON at the beginning of the light pulse to preset the comparators and turned OFF typically 5  $\mu s$  after the end of the light pulse, providing thus a comparison when the input currents are close to their peak value (Fig. 5). When the pixel current is either smaller or bigger than the neighbor photocurrent by a given factor, logic combinations of the comparators output by three NAND’s signal the presence of a vertical edge ( $E_x$ ) between the pixel photodiode and its right neighbor, respectively, a horizontal edge ( $E_y$ ) between the pixel photodiode and its upper neighbor. The sign of the gradient of the edge seen from the pixel ( $S$ ) is also determined to differentiate between negative and positive edges at two

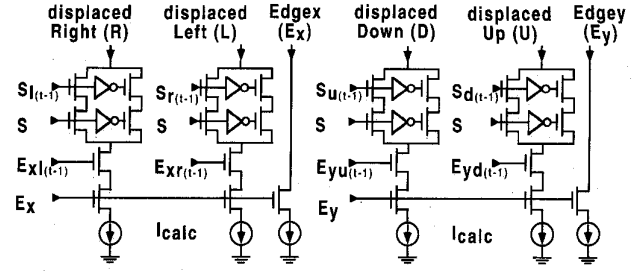


Fig. 6. Local computation of motion.

consecutive light pulses. The three latched current comparators hold the information about the position of the edges after light is off. Before each light pulse, information about edges at the previous pulse has therefore to be shifted in three latches controlled by the signal “Shift,” to hold  $E_{x(t-1)}$ ,  $E_{y(t-1)}$ , and  $S_{(t-1)}$ .

### C. Local Displacement Estimate

Between light pulses, a switch-logic block (Fig. 6) computes the local estimate of the displacement of a vertical edge ( $E_x$ ) to the right ( $R$ ) or to the left ( $L$ ). Respectively, a similar block computes the local estimate of the displacement of a horizontal edge ( $E_y$ ) in the up ( $U$ ) or down ( $D$ ) directions. This computation is simply done by correlating the information about edges and their sign at time  $t$  in the pixel with the information at  $t - 1$  in the neighbors. For example, on a given pixel, an edge  $E_x$  with a gradient sign  $S$  is signalled to have moved right if an edge with the same gradient was signalled on the left pixel at time  $t - 1$  ( $E_{xl(t-1)} = E_{xr(t)}$  and  $S_{l(t-1)} = S_{(t)}$  is then true). To simplify the implementation of the sum ( $\sum$ ) in (1) and (2), the circuit injects a current of 100 nA when the corresponding output ( $E_x$ ,  $E_y$ ,  $R$ ,  $L$ ,  $D$ , and  $U$ ) is true on the respective wire of a six-line analog bus. Each pixel feeding the bus in parallel, the total current value on each wire carries respectively the sum of edges moving in one of the four directions ( $\sum R$ ,  $\sum L$ ,  $\sum U$ ,  $\sum D$ ) and the total number of edges present in the  $x$  and  $y$  orientations ( $\sum E_x$  and  $\sum E_y$ ) at time  $t$ . The current is generated on-chip by a current reference block (Fig. 1). Its value needs to be high enough to drive the following stages in the specified time, but does not need to be precise since only current ratios are computed in the following stages.

### D. Global Displacement Calculation

The previous six-current values are processed outside the matrix to compute  $\Delta x/P$  and  $\Delta y/P$  according to (1) and (2). Two absolute-value circuits implement the numerator of (1) and (2), respectively (Fig. 7). They detect the sign of the difference (motion direction) and accordingly swap positive and negative inputs to achieve the absolute value which is fed to two A/D converters. Multiplying algorithmic A/D converters [9] operating in the current mode compare the absolute values to fractions of  $\sum E_x$ , respectively  $\sum E_y$ , to output a 4-b digital word which, combined with their respective sign, feeds the external microprocessor serially. The

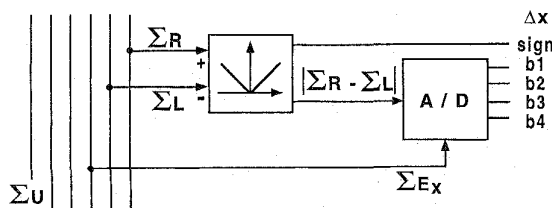


Fig. 7. Global displacement calculation.

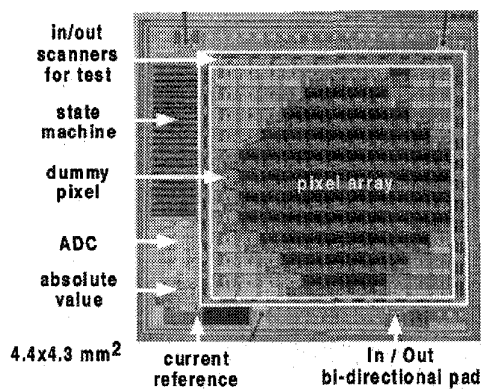


Fig. 8. Chip micrograph.

state machine (Fig. 8) controls the communication protocol and provides signals for the pixel matrix during normal operation as well as during the test procedure.

#### E. On-Chip Test

Because it is not practical with modern test equipment to focus an image onto the chip during on-wafer test procedure, each pixel is tested on-chip by injecting a current  $I_{test}$  in parallel with the output of the current amplifier (Fig. 9). A current reference is implemented on-chip in order to limit input/output test vectors to digital values. Using two shift registers (one for column and one for row) controlled by the state machine, a sequence of patterns simulating image displacements is injected into the matrix and serves as basis to test analog and digital processing blocks in each pixel, as well as the global calculation block (absolute value circuit and A/D converter). Means to scan out the digital values of  $E_x$ ,  $E_y$ , and  $S$  and the analog values of the photodetectors have also been implemented on-chip to allow for proper characterization and debugging during the design phase.

#### V. PERFORMANCE SUMMARY AND CONCLUSION

The chip ( $4.4 \times 4.3 \text{ mm}^2$  without scribe lines) has been implemented in a  $2\text{-}\mu\text{m}$  CMOS low-power and low-voltage technology to allow an operating voltage range of 2.4 to 5.5 V. Fig. 8 shows a micrograph of the circuit implementing image acquisition and displacement estimation. The pixel matrix is laid out in a round shape corresponding to the optics field of view. Thanks to the use of a bidirectional in/out pad, only four pads are needed (two for supply voltages, one for clock

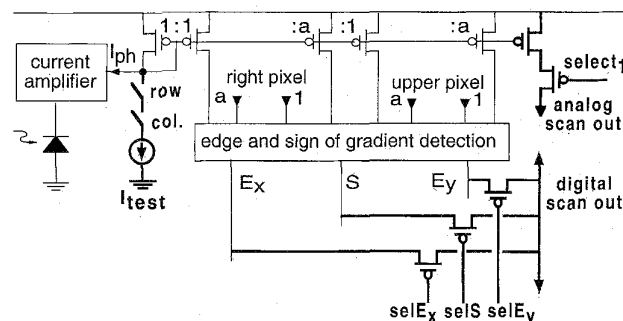


Fig. 9. On-chip test.

and one for data in/out). For a given ball with a random pattern printed on its surface and for illumination ranges of  $100\text{--}2000 \text{ mW/m}^2$ , experimental results show that the motion detector system is able to detect ball movements in the range of  $0\text{--}11.8 \text{ in/s}$  with a resolution higher than 800 dpi. The current consumption is smaller than  $25 \mu\text{A}$  in the idle mode, which corresponds to most of the pointing device operating time, and can be decreased below  $3 \mu\text{A}$  in a sleep mode. Only 75 pixels, each containing a photoreceptor and local processing circuits (38 analog and 102 digital transistors) are needed for the specified resolution. When some of the 75 pixels are not functional or part of the image is covered by dust, resolution decreases as a function of the number of nonworking pixels, since its value depends on the number of edges detected by the photosensitive matrix at a given time.

The image sensor presented here shows an example of the processing capabilities offered in particular by analog VLSI [10]. Exploiting parallel local information and global aggregation of that information provides subpixel resolution and graceful degradation properties as well as a dense chip implementation, resulting in an industrial attractive solution.

#### ACKNOWLEDGMENT

The authors thank E. A. Vittoz for his constant support throughout the project, as well as P. Heim for many helpful comments.

#### REFERENCES

- [1] R. F. Lyon, "The optical mouse and an architectural methodology for smart digital sensors," in *CMU Conf. VLSI Systems Computations*, 1981, pp. 1–19.
- [2] R. A. Sprague, "Optical cursor control device," U.S. Patent 4409 479, Oct. 11, 1983.
- [3] J. Tanner and C. A. Mead, "Correlating optical motion detector," U.S. Patent 4 631 400, Dec. 23, 1986.
- [4] J. Tanner, "Integrated optical motion detection," Ph.D. dissertation, California Institute of Technology, Pasadena, CA, 1986.
- [5] M. Gottardi and W. Yang, "A CCD/CMOS image motion sensor," in *Dig. Tech. Papers, ISSCC'93*, San Francisco, p. 193.
- [6] R. C. Meitzler, K. Strohhahn, and A. G. Andreou, "A silicon retina for 2-D position and motion computation," in *Proc. 1995 Int. Symp. Circuits Systems*, Seattle, WA, June 1995, vol. III, pp. 2096–2099.
- [7] R. Sommer, "Low-power optoelectronic device and method," U.S. Patent Application Ser. no. 07/717,187, June 18, 1991.
- [8] C. C. Enz, F. Krummenacher, and E. A. Vittoz, "An analytical MOS transistor model valid in all regions of operation and dedicated to low-voltage and low-current applications," Special Issue of the *Analog*

*Integrated Circuits and Signal Processing J. Low-Voltage and Low-Power Design*, Kluwer, vol. 8, pp. 83–114, July 1995.

- [9] D. Nairn, "Algorithmic and pipelined A/D converters," in *Switched-Currents: An Analogue Technique for Digital Technology*, C. Tomazou *et al.* Eds. London: Peregrinus, 1993.
- [10] C. A. Mead, *Analog VLSI and Neural Systems*. Reading, MA: Addison-Wesley, 1989.



**Xavier Arreguit** was born in Oviedo, Spain, in 1961. He received the M.S. and Ph.D. degrees in electrical engineering from the Swiss Federal Institute of Technology in Lausanne (EPFL) in 1985 and 1989, respectively.

After a Postdoc at the California Institute of Technology (Caltech), he joined the Centre Suisse d'Electronique et de Microtechnique S.A. (CSEM) in July 1991 where he is presently involved as a Project Manager in the division of Advanced Research and Development. His main interests include

analog VLSI for perceptive systems.



**F. André van Schaik** (S'94) received the M.S. degree in electrical engineering from the Technical University of Twente in 1990.

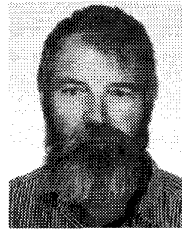
From 1991 to 1993 he worked as a Scientific Staff Member at the Centre Suisse d'Electronique et de Microtechnique S.A. (CSEM) in the field of analog VLSI chips for perceptive tasks. Since 1994, he is a research assistant and Ph.D. student at the MANTRA Centre for Neuro-Mimetic Systems of the Swiss Federal Institute of Technology in Lausanne (EPFL) working on the development of

biological inspired analog VLSI for audition (hearing).



**François V. Bauduin** was born in Charleroi, Belgium, on August 8, 1984. He received the M.S. degree in electrical engineering from the University of Liege, Belgium, in 1987.

In 1990 he joined the Centre Suisse d'Electronique et de Microtechnique S.A. (CSEM). He is now involved in the design of analog and digital circuits, with emphasis on low-power telecommunication applications.



**Marc Bidiville** was born in Lausanne, Switzerland, in 1948. He received the M.S. degree in electrical engineering from the Swiss Federal Institute of Technology in Lausanne (EPFL) in 1971.

In 1981, he joined Logitech as a co-founder where he is now a Consulting Director. His main interests include optical sensors and microsystems development and production.



**Eric Raeber** was born in Koln, Germany, in 1967, with Swiss nationality. He received his EPFL diploma in E.E. in 1991.

Since then he worked three years for Logitech Switzerland, developing the Marble technology in collaboration with CSEM. He has then been transferred to Logitech USA where he leads software projects for pointing devices.